Chemical Engineering Journal 155 (2009) 567–579

Contents lists available at ScienceDirect

Chemical Engineering Journal

journal homepage: www.elsevier.com/locate/cej

# Multistage optimization of the adsorption of methylene blue dye onto defatted Carica papaya seeds

Emmanuel I. Unuabonah*, Gilbert U. Adie, Lora O. Onah, Olalere G. Adeyemi

*Department of Chemical Sciences, College of Natural Sciences, Redeemer's University, Km 46, Lagos-Ibadan Expressway, Redemption city, Ogun State, Nigeria*

ARTICLE INFO

*Article history:*
Received 2 April 2009
Received in revised form 22 June 2009
Accepted 1 July 2009

*Keywords:*
Surface chemistry
Kinetic rate
Optimization
*Carica papaya*
Adsorption stages
Methylene blue

ABSTRACT

*Carica papaya* seeds were defatted and used for the adsorption of methylene blue dye (MB dye). The $pH_{PZC}$ and specific surface area (SSA) of the defatted and undefatted Carica papaya seeds were found to be 6.25 and 143.27 $m^2\ g^{-1}$ respectively. The adsorption capacities of the defatted Carica papaya seeds were 1250 and 769.23 $mg\ g^{-1}$. Fourier transformed infrared (FT-IR) spectra analysis of defatted seeds suggests the presence of α,β-unsaturated ketone, β-keto (enolic) esters and lactones, quinones and carboxylic acids which were absent in the undefatted sample. The presence of carboxylic acid, phenolic and lactone functional groups were confirmed by surface chemistry studies. Adsorption of MB dye onto DPS adsorbent was found to be exothermic and spontaneous. FT-IR spectra of various particle sizes indicate the presence of functional groups on every particle size necessary for the adsorption of MB dye.

Pseudo-second-order kinetic rate constant increased with increasing initial MB dye concentration. The adsorption reaction was observed to be very fast perhaps because of the presence of multiple functional groups with some of them having lone pair of electrons. Increasing pH was observed to have very little positive effect on the adsorption of MB dye on DPS adsorbent. Increasing particle size decreased the adsorption capacity of DPS adsorbent for MB dye. It is suggested that the mechanism for the adsorption of MB dye onto DPS adsorbent might not only be solely controlled by film diffusion but also by pore diffusion.

Mathematical models for the optimization of adsorbent dose, number of adsorption stages and minimum contact time were developed. The optimum conditions for the adsorption of 99% of 100 $mg\ L^{-1}$ MB dye from 10 $m^3$ of aqueous solution of the dye were five adsorption stages, ≈21 kg for each stage with a total minimum contact time of ≈71 min.



## 1. Introduction

The problem of colour removal from pulp-and-paper mill waste, pharmaceuticals and from textile industries has been a subject of great consideration and investigation in the last few decades. Some specific effluents from industrial production processes may be difficult to purify by traditional wastewater treatment technology, as a result of the complexity of some of their components. Wastewater from textile industries creates a great problem of pollution due to the dyes contained therein. The disposal of coloured wastes such as dyes into receiving waters causes damage to the environment as they are toxic to aquatic life. Thus, because of the difficulties experienced in removing the dyes from effluents, different adsorbent have been used for this purpose [1].

There are many treatment processes applied for the removal of dyes from wastewater. A critical review on current treatment technologies with a proposed alternative was reported by Robinson et al. [2]. Some materials that have been used for the adsorption of dyes includes orange peels [3], Sepiolite [1], bagasse fly ash [4], zeolite [5] boiled *Carica papaya* seeds [6], etc.

In the world today, *Carica papaya* (*Carica papaya* L.) production ranks 10th among all fruit species grown for commercial purpose. This is closely followed by Citrus (*Citrus* spp.), bananas (*Musa* spp.) grapes (*Vitis* spp.) apples (*Malus* spp.), mangoes (*Mangifera indica* L.) pineapples (*Ananas comosus Merr.*) pears (*Pyrus* spp.) and peaches (*Prunus* spp.) [7]. In 2002, Nigeria was ranked among the other countries like Brazil, Indonesia, and India, as a world *Carica papaya* producer [8].

In Nigeria, *Carica papaya* fruit is a delicacy which is usually eaten with or without meals. The seeds are often times discarded as waste. The fruits have tremendous nutritional value and contain 1.5% protein, 0.1% fat, 7.1% carbohydrates, and 35.0 calories per 100 g edible fruit. They also contain high levels of calcium, iron, sodium, potassium, β-carotene, vitamin B2, niacin, and vitamin C [9–11].

*Carica papaya* seeds, the fruits, leaves, and latex are used medicinally. The main medicinal use of *Carica papaya* seeds is as a digestive agent. It is prescribed for people who have difficulty digesting pro-

* Corresponding authors. Tel.: +234 805 3175 971.
*E-mail addresses:* iyaemma@yahoo.com (E.I. Unuabonah), adeyemio@run.edu.ng (O.G. Adeyemi).

1385-8947/$ – see front matter © 2009 Elsevier B.V. All rights reserved.
doi:10.1016/j.cej.2009.07.012

tein and is also used to break up blood clots after surgery, this is due to the presence of enzyme papain in the plants latex [12]. The seeds are reported to contain 24.3 g protein, 25.3 g fatty oil, 32.5 g total carbohydrate, 17.0 g crude fiber, 8.8 g ash, 0.09 g volatile oil, a glycoside, caricin, and the enzyme, myrosin per 100 g of the seeds. The fatty oil of the seeds contains 16.97% saturated acids (11.38% palmitic, 5.25% stearic, and 0.31% arachidic) and 78.63% unsaturated acids (76.5% oleic and 2.13% linoleic). With reversed-phase partition column chromatography, the oil from the seeds of *Carica papaya* was found to contain the following acids: lauric, 0.4%; myristic, 0.4%; palmitic, 16.2%; stearic, 5.0%; arachidic, 0.9%; behenic, 1.6%; hexadecenoic, 0.8%; oleic, 74.3%; and linoleic, 0.4% [13]. It has been concluded that papaya seed oil is a potential source of high oleic oil and its full potential should be exploited [14].

Recently Hameed [6] reported the use of boiled *Carica papaya* seeds in the adsorption of methylene blue (MB) dye with an adsorption capacity of 555.557 mg $g^{-1}$ while Bashaa et al. [15] used the trunk for the adsorption of mercury (II) with an adsorption capacity of 155.6 mg $g^{-1}$. These suggest the future potential of the plant in the removal of organics and metals from aqueous solution.

However, because of the usefulness of the lipids in the seeds as mentioned earlier, this research reports the use of defatted *Carica papaya* seeds for the adsorption of methylene blue (MB) dye from aqueous solution. Some variables that affect adsorption capacity of DPS adsorbent such as particle size, pH, adsorbent dose, initial dye concentration, temperature, and time were studied.

In the recent past, the two-stage batch adsorption models have been used in the optimization of kinetic or equilibrium data from a one-stage batch adsorption process. However, no attempt has been made to first optimize the number of adsorption stages before optimizing contact time. This study further provided mathematical models and data for the optimization of the number of adsorption stages and minimum contact time for the adsorption of MB dye onto DPS adsorbent (defatted *Carica papaya* seeds). The minimum contact time for the optimized number of adsorption stages was also reported. These would be useful for the design and use of an adsorption system for MB dye adsorption.

## 2. Materials and methods

### 2.1. Preparation of DPS adsorbent

The seeds of *Carica papaya* were collected from the open markets in Benin City, Nigeria and left under the sun to dry. After 7 days, the seeds were collected and crushed. The crushed seeds were then defatted using the soxhlet extraction method using hexane. The defatted sample of *Carica papaya* was collected and dried in a fume hood to allow residual hexane to go off the sample. The sample collected thereafter is therefore referred to as defatted *Carica Papaya* seeds (DPS).

### 2.2. Surface chemistry of DPS adsorbents

Surface chemistry of the DPS adsorbent was characterized by adopting Boehm titration and pH drift (or $pH_{pzc}$—pH of point of zero charge). Boehm titration method is described as follows: 0.5 g of well ground DPS were dispersed in duplicate in 50 mL each of 0.05 M $NaHCO_3$, 0.025 M $Na_2CO_3$, 0.05 M NaOH and 0.05 M HCl contained in 250 mL capacity glass bottles with tight glass corks. The bottles were shaken using an end-to-end shaker at 180 rpm for 24 h. After 24 h, the samples were filtered using whatman No.1 filter paper and titrated with 0.05 M NaOH or 0.05 M HCl depending on the starting solution used. The amount of acidic groups on the surface of the DPS adsorbent were approximately probed as follows: $NaHCO_3$ (carboxylic group), $Na_2CO_3$ (carboxylic and lactonic groups) and NaOH (carboxylic, lactonic and phenolic groups). The number of surface basic sites was calculated from the amount of HCl that reacted with the filtrate.

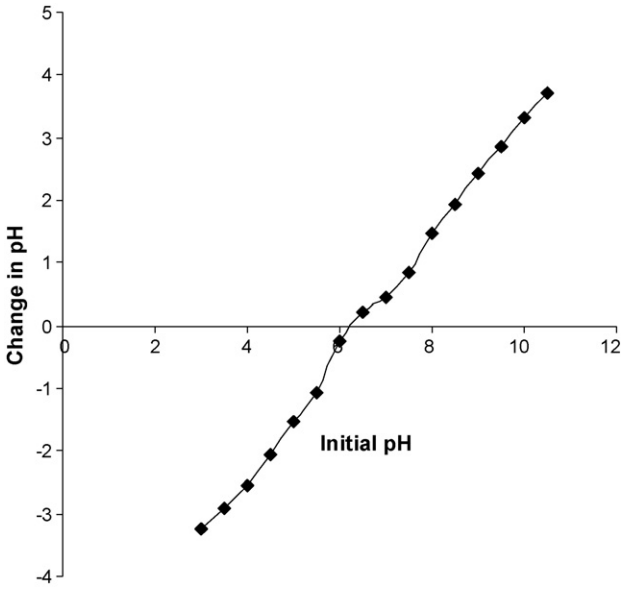


**Fig. 1.** $pH_{pzc}$ plot for adsorption of MB dye onto DPS adsorbent.

The method used for $pH_{pzc}$ of DPS adsorbent was a modification of [16]. The method is described as follows: 50 mL of 0.01 M KCl were prepared and added into a series of glass bottles with corks. Their pH values were adjusted in range between 2 and 12 at interval of 0.5 using either 0.01 M HCl or 0.01 M NaOH. The pH of initial solutions were measured with a pH meter and noted as $pH_{initial}$. After constant value of $pH_{initial}$ had been reached; 0.15 g of the ground DPS sample was added to each bottle and then corked. This set up was shaken for 48 h. After 48 h, the second pH of the extracts noted as $pH_{final}$ was measured with a pH meter. A plot of $pH_{initial}$ on the *x*-axis against the difference between $pH_{initial}$ and $pH_{final}$ on the *y*-axis was made as shown in Fig. 1. $pH_{PZC}$ was the point where the curve cuts the *x*-axis implying the point when $pH_{initial} = pH_{final}$.

The specific surface area (SSA) of DPS adsorbent was calculated from the following equation [17]:

$$S_{MB} = \frac{N_g \times a_{MB} \times N \times 10^{-20}}{M} \quad (1)$$

where $S_{MB}$ is the specific surface area in $10^{-3}$ $km^2$ $kg^{-1}$; $N_g$ is the number of molecules of MB dye adsorbed at the monolayer of fibers in kg $kg^{-1}$ (or $N_g = N_m M$); $a_{MB}$ is the occupied surface area of one molecule of MB dye = 197.2 $Å^2$ [18]; $N$ is Avogadro's number, $6.02 \times 10^{23}$ $mol^{-1}$; and $M$ is the molecular weight of MB dye, 373.9 g $mol^{-1}$. This method has been proven to be as efficient as the BET and ethylene glycol monoethyl ether (EGME) methods of determining SSA [19–23].

### 2.3. Infrared spectroscopy

The technique of Devarly et al., used in [16] was used with slight modification. The vibrational frequencies of both defatted and undefatted *Carica papaya* seeds were obtained from FT-IR transmission spectra of defatted and undefatted seeds by KBr method. The grinded KBr powder was pressed with SHIMADZU MHP-1 mini hand press to form homogenized pellet for background measurement. A 10% dilution of either defatted or undefatted *Carica papaya* crushed seeds with KBr was grinded with agate mortar to have a homogenized mixture. A pellet suitable for FTIR measurement was

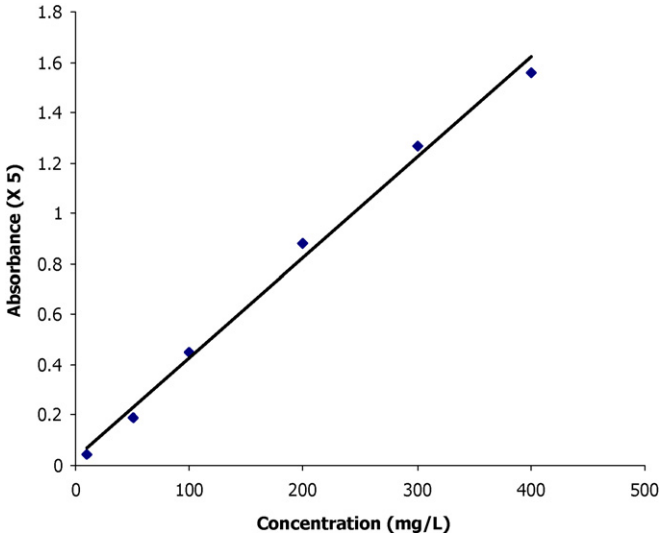


**Fig. 2.** Calibration curve for the adsorption of MB dye onto DPS adsorbent.

produced using the SHIMADZU MHP-1 mini hand press. The sample measurement was taken in the percent transmittance mode. SHIMADZU 8400S FT-IR instrument in the vibrational absorption range of 4000–500 $cm^{-1}$ was employed. This same method was employed for the FTIR study of the various particle sizes of the defatted *Carica papaya* samples.

### 2.4. Adsorption study

A stock solution of 1000 mg $L^{-1}$ MB dye was prepared. Various concentrations (10–400 mg $L^{-1}$) of the MB dye were prepared from stock solution and were read on a UV–vis spectrophotometer. A calibration curve of absorbance against MB dye concentrations was obtained by using standard MB dye solutions of known concentrations (in the range of 10–400 mg $L^{-1}$) at pH values between 7.04 and 7.5. The experimental data reported in Fig. 2 were fitted by a straight line with a high correlation coefficient ($r^2$ = 0.9931). The high value of the correlation coefficient of the calibration line observed in the present study allows us to consider that the molar absorptivity is constant over the concentration range investigated. Thus, the MB dye concentration will be determined with good precision [24].

Thereafter, the plot was used subsequently to determine the equilibrium concentration of samples collected. In determining the effect of concentration of the adsorption capacity of DPS adsorbent, a range of concentration from 10 to 400 mg $L^{-1}$ were prepared and 50 mL of each were poured into an amber bottle (amber bottles were used so as to reduce the intensity of light reaching the solution) dye solutions containing 0.5 g of DPS adsorbent. The mixtures were agitated on a shaker (Grants Instrument Ltd., England) for 2 h at 180 rpm and 298 K after which the solutions were filtered and the filtrates were immediately analyzed for concentration of MB dye using a UV–vis spectrophotometer.

To study the effect of temperature on the adsorption of MB dye onto DPS adsorbent, the procedure above was repeated at 313 and 323 K. The thermodynamic parameters, $\Delta H$, $\Delta S$ and $\Delta G$, for the adsorption process are calculated using the relation:

$$\ln b = \frac{\Delta S}{R} - \frac{\Delta H}{RT} \tag{2}$$

where $b$ is the Langmuir constant related to energy, $R$ is gas constant and $T$ is the absolute temperature (K), $\Delta H$ is the enthalpy of the adsorption (kJ $mol^{-1}$), $\Delta S$ is the entropy of the adsorption process (J $mol^{-1}$). The plot of $\ln b$ versus $1/T$ yields straight lines with the slope and the intercept giving values of $\Delta H$ and $\Delta S$. These values could be used to compute $\Delta G$ from the Gibbs relation, $\Delta G = \Delta H - T\Delta S$ at constant temperature. In deriving the values of the thermodynamic parameters, it is assumed that the enthalpy does not change with temperature.

For the effect of adsorbent dose, various weights of the DPS adsorbent ranging from 0.5 to 2.0 g were weighed into amber bottles and 50 mL of 100 mg $L^{-1}$ MB dye were subsequently added to them. These mixtures were agitated for 2 h at 180 rpm at 298 K. The mixtures were then filtered with whatman No. 1 filter paper. The concentrations of MB dye in filtrates were read from a UV–vis spectrophotometer. The same procedure was followed for the study on the effect of pH on adsorption. The pH of the 100 mg $L^{-1}$ adsorbate solution was varied from 4 to 10 and the weight of DPS adsorbent used was 0.5 g. The pHs of the various solutions were adjusted using 0.1 M NaOH and 0.1 M $HNO_3$ with Omega PHB-212 microprocessor pH meter.

Four different sizes (75, 300, 500 and 750 μm) of DPS adsorbent were introduced into separate amber bottles containing 10, 50, 100 and 200 mg $L^{-1}$ of MB dye in a 50 mL standard flask solution. To each solution 0.5 g of a certain particle size of DPS adsorbent was added. The mixtures were agitated for 2 h at 180 rpm at 298 K. Thereafter, the filtrates were immediately analyzed for MB dye using a UV–vis spectrophotometer.

### 2.5. Kinetic study

Three different concentrations (50, 100 and 200 mg $L^{-1}$) of MB dye were prepared and added to 0.5 g of DPS adsorbent in ambered bottles. These were agitated at 180 rpm at 298 K. Samples were taken out of the shaker at different time intervals. The samples were then filtered and the filtrates were immediately analyzed for MB dye using a UV–vis spectrophotometer.

Kinetic data were further used to investigate the slow step occurring in the present adsorption system using Bangham's equation [25]:

$$\log\left(\log\left(\frac{C_0}{C_0 - q_t m}\right)\right) = \log\left(\frac{k_o m}{2.303V}\right) + \alpha\ \log(t) \tag{3}$$

where $V$ is the volume of solution (L) and $\alpha$ (<1) and $k_o$ (g) are constants, m is the weight (g) of DPS adsorbent used for the adsorption reaction, and $t$ is time (min).

Other kinetic models used for the analysis of kinetic data include:

- The pseudo-first-order model (PFOM) which is obtained as follows

$$\frac{dq_t}{dt} = k(q_e - q_t) \tag{4}$$

On rearrangement

$$\frac{dq_t}{q_e - q_t} = kdt$$

which on integration under the boundary conditions of $t = 0$ to $t$, and $q_t = 0$ to $q_t$, gives a linear logarithmic expression,

$$-\ln(q_e - q_t) + \ln\ q_e = k_t \tag{5}$$

- The pseudo-second-order kinetic model (PSOM) which is obtained as follows:

$$\frac{dq_t}{dt} = k_2(q_e - q_t)^2 \tag{6}$$

On rearrangement and integration

$$\frac{1}{q_e - q_t} - \frac{1}{q_e} = k_2 t \tag{7}$$

**Table 1**
Values of surface acidity and $pH_{PZC}$ of DPS adsorbent using Boehm's titration.

| Sample | Carboxylic | Lactonic | Phenolic | Acidic value | Basic value | pH | $pH_{PZC}$ |
|---|---|---|---|---|---|---|---|
| | mequiv./g of DPS adsorbent | | | | | | |
| DPS adsorbent | 0.098 ± 0.013 | 0.117 ± 0.009 | 1.864 ± 0.022 | 2.078 | 0.587 | 7.05 | 6.25 |

When this is linearized, it gives

$$\frac{t}{q_t} = \frac{1}{k_2 q_e^2} + \frac{t}{q_e} \quad (8)$$

where $q_e$ is the amount of MB dye adsorbed at equilibrium (mg g$^{-1}$), $q_t$ is the amount of MB dye adsorbed at time $t$ (min) in mg g$^{-1}$ and $k_2$ is the rate constant of the PSOM for sorption of both metal ions.

The initial sorption rate $h$, can be obtained by the following equation:

$$h = k_2 q_e^2$$

where $h$ is the initial sorption rate (mg (g min)$^{-1}$).

$$q_t = \frac{k_2 q_e^2 t}{1 + k_2 q_e t} \quad (9)$$

All MB dye sample solutions were read at 668 nm using Spectrumlab 23A Spectrophotometer made by Easy Way Medical England.

### 2.6. Adsorption isotherms

The Langmuir isotherm is a valid monolayer sorption on a surface containing a finite number of binding sites. It assumes uniform energies of sorption on the surface and no transmigration of adsorbate in the plane of the surface. The Langmuir equation may be written as

$$q_e = \frac{Q^o b C_e}{1 + bC_e} \quad \text{(non-linear form)} \quad (10)$$

$$\frac{1}{q_e} = \frac{1}{Q^o b C_e} + \frac{1}{Q^o} \quad \text{(linear form)} \quad (11)$$

where $q_e$ is the amount of solute adsorbed per unit weight of adsorbent (mg g$^{-1}$), $C_e$ is the equilibrium concentration of solute in the bulk solution (mg L$^{-1}$), $Q^o$ is the monolayer adsorption capacity (mg g$^{-1}$) and $b$ is the constant related to the energy of adsorption (L g$^{-1}$). It is the value reciprocal of the concentration at which half the saturation of the adsorbent is attained.

The other equilibrium isotherm models were used for adsorption data fittings Freundlich isotherm model

$$q_e = K_F C_e^{1/n} \quad (12)$$

$$\log\ q_e = \log K_f + \frac{1}{n} \log C_e \quad (13)$$

The nonlinear chi-square error method of analysis was used to fit experimental $q_t$ data against theoretical $q_t$ data. The equivalent mathematical statement for the nonlinear chi-square as given by [26] is:

$$\chi^2 = \sum \frac{(q_e - q_{e,m})^2}{q_{e,m}} \quad (14)$$

where $q_{e,m}$ is equilibrium capacity obtained by calculating from the model (mg g$^{-1}$) and $q_e$ is experimental data of the equilibrium capacity (mg g$^{-1}$). If data from model are similar to the experimental data, $\chi^2$ will be small in number, while if they differ, $\chi^2$ will be a bigger number.

## 3. Results and discussions

### 3.1. Surface chemistry

The surface of DPS adsorbent contains heteroatom like hydrogen, oxygen, nitrogen, sulphur, halogen and phosphorus [16]. These atoms to a very great extent determine the surface chemistry of the seeds. Surface chemistry study is basically done to probe the acidity and basicity of the material under study. The presence of surface functional groups like carboxylic, lactonic and phenolic groups are known to constitute the acidity of the material while oxygen containing groups and oxygen free Lewis basic sites constitute the basicity.

Table 1 highlights the quantitative surface chemistry analyses of DPS adsorbent consisting of the amount of acidic and basic functional groups. The pH at which the $H^+$ and $OH^-$ were equal, known as the pH at point of zero charge ($pH_{PZC}$), was also determined (Fig. 1). The acidic $pH_{PZC}$ of 6.25 shown by the DPS adsorbent is consistent with the Boehm titration result that presented dominance of acidic group of the surface of the seeds. This is in accordance with [1,27] who observed the same trend on activated carbon fiber samples and activated carbon from jackfruit peel waste, respectively.

The specific surface area, $S_{MB}$, of DPS adsorbent was found to be 143.27 m$^2$ g$^{-1}$. This specific surface area is large when compared with lignocellulosic substrate (185 m$^2$ g$^{-1}$) [28], prawn pond algae treated with acid (2.1 m$^2$ g$^{-1}$) [29], pure wild cocoyam biomass (32.91 m$^2$ g$^{-1}$) [30], palm shell powder (2.52 m$^2$ g$^{-1}$) [31], powder orange peel (128.7 m$^2$ g$^{-1}$) [32] and other biosorbents used for adsorption recently.

### 3.2. Infrared spectroscopy analysis

Fig. 3 shows the FT-IR spectra of defatted and Undefatted Carica papaya seeds in the range of 4000–500 cm$^{-1}$. Several distinct and sharp absorptions were observed as well as relatively low intensity peaks for both defatted (DPS adsorbent) and undefatted (UDPS) sample spectra. The wave number in the range of 3480–3440 cm$^{-1}$

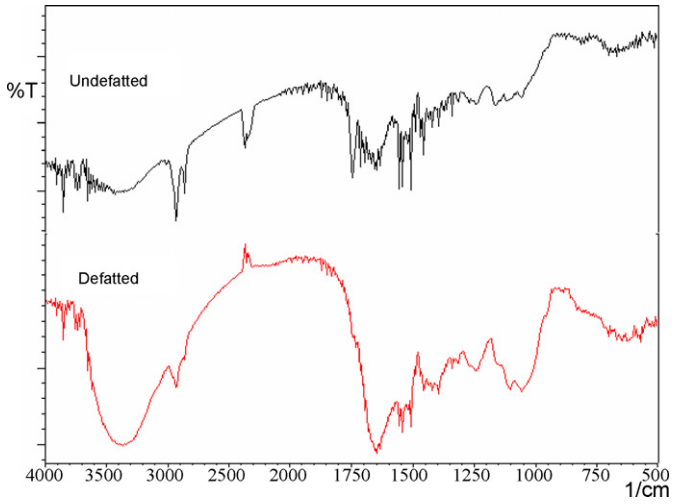


**Fig. 3.** Fourier transformed infrared spectra for defatted (DPS) and undefatted (UDPS) adsorbents.

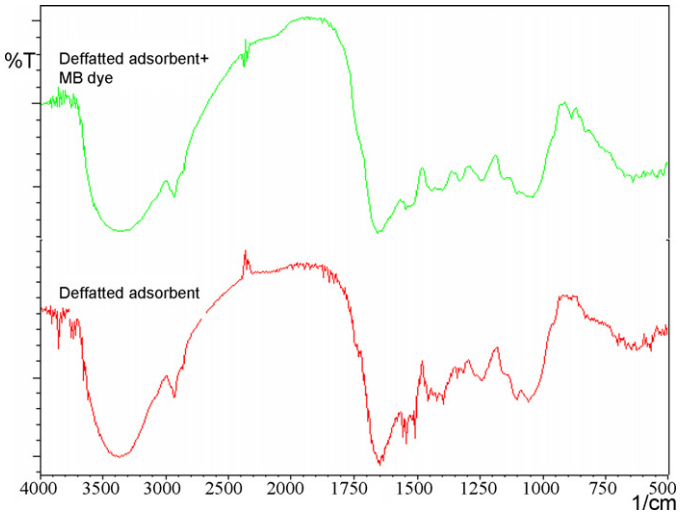


**Fig. 4.** Fourier transformed infrared spectra for defatted (DPS) and defatted + MB dye adsorbents.

is N–H stretch associated with N-substituted amide. The medium absorption band at 2930 and 2380 $cm^{-1}$ are the $\nu_{C-H}$ stretching and $\nu^{2+}_{=N-H}$ group, respectively. It should be noted that, the absorption band around 2850 $cm^{-1}$ in the Undefatted spectra disappeared in the defatted spectra. This could be associated with C–H stretching vibration of methyl substituent in the lipid. A medium band around 1700 $cm^{-1}$ in the Undefatted spectrum is $\nu_{C=O}$ stretching, an indication of the presence of aldehyde coupled with the band around 2800 $cm^{-1}$ (C–H stretching from the aldehyde). In the defatted spectrum, a sharp and distinct absorption was observed at 1650 $cm^{-1}$ (C=O stretching). This is clear indication of the presence of α,β-unsaturated ketone, β-keto (enolic) esters, Lactones, quinones and carboxylic acids. Medium band at 1630 $cm^{-1}$ in the Undefatted spectrum which is an indication of amide band I bond in N-acetyl glucosamine polymer or protein peptide bond [15] disappeared in the defatted spectrum. Peaks around 1040 $cm^{-1}$ is S=O vibrational frequency. The peaks were observed in both spectra. It is evidenced that there are some differences in the functional groups of the defatted and Undefatted Carica papaya seeds.

The FT-IR spectra of DPS and DPS + MB dye adsorbents are shown in Fig. 4.

The two spectra are similar with slight shift in some characteristic absorbance peak. The approximate absorption bands in DPS adsorbent shifted at 3344, 1654, 1539, and 1515 $cm^{-1}$ when it absorbed MB dye as against the approximate absorption at 3387, 1647, 1553 and 1503 $cm^{-1}$ without the dye on it (i.e. the DPS adsorbent without MB dye). This suggests that amides, carboxylic acids and aromatic double bonds are available for bonding. The ligational directions of MB dye with DPS adsorbent may be complex because it consists of secondary amines and mercaptan which possess readily available lone pairs of electron for bonding onto the DPS adsorbent.

Fig. 5 shows the FT-IR spectra for the various particle sizes of DPS adsorbent. The spectra suggest that all particle sizes have the same type of the functional groups hence adsorption sites.

### 3.3. Effect of adsorbent dose

Fig. 6 shows the relationship between DPS adsorbent dose and percentage MB dye adsorbed. It was observed that increasing dosage of DPS adsorbent increased the percentage MB dye adsorbed although at the least liquid–solid ratio (50 mL: 0.05 g) there was a large percentage of MB dye adsorbed (≈98%) for the adsorption of 100 mg $L^{-1}$ of MB dye. However, a reverse trend was observed with adsorption capacity, $q_e$, as increased adsorbent dose from 0.05 to

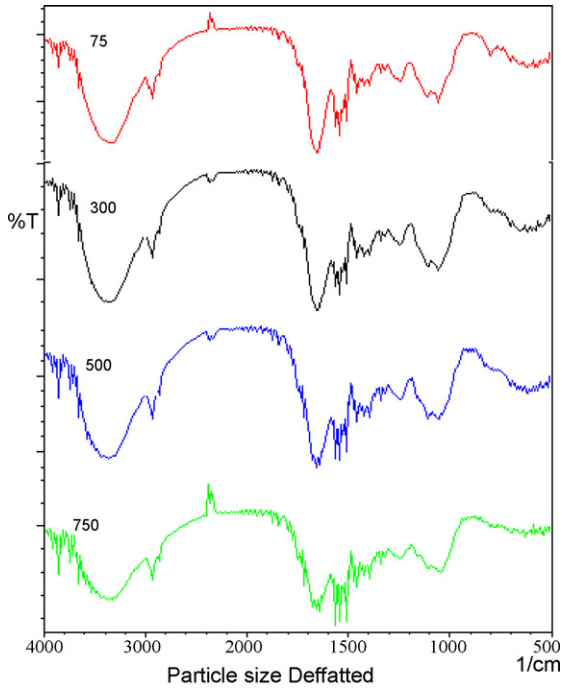


**Fig. 5.** Fourier transformed infrared spectra for the various particle sizes of defatted (DPS) adsorbent in μm.

1.0 g led to a decreased adsorption capacity of DPS adsorbent for the adsorption of MB dye from 98.19 to 2.5 mg $g^{-1}$. The increased percentage adsorption of MB dye onto DPS adsorbent was as a result of increased surface area and increased adsorption site occasioned by increased adsorbent dose. The same trend has been observed by Hameed [6]. However, the observed decrease in adsorption capacity may be due to decrease in liquid–solid ratio from 1 to 0.025 (from 0.05 to 1.0 g in 0.05 L MB dye).

### 3.4. Effect of pH

The effect of pH on the adsorption of MB dye onto DPS adsorbent is shown in Fig. 7. With change in pH from 4.0 ± 0.02 to 10 ± 0.03 there was no significant increase in the adsorption capacity of DPS adsorbent. This was also observed by Hameed [6] in the adsorption of MB dye onto boiled *Carica papaya* seeds. There was a

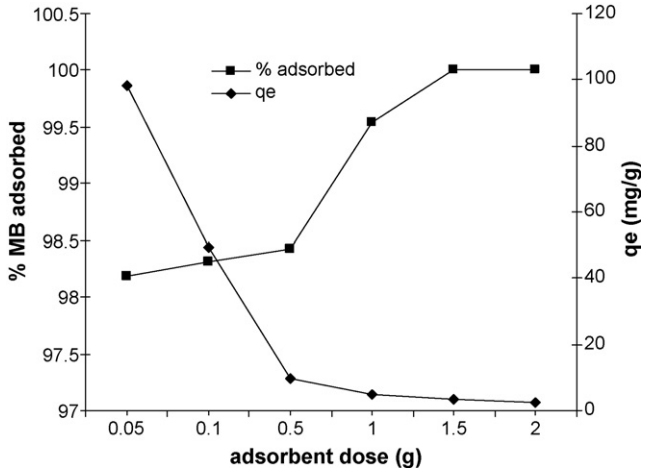


**Fig. 6.** Effect of DPS adsorbent on the adsorption of MB dye onto DPS adsorbent (adsorbent dose: 0.05 mg $L^{-1}$ to 2.0 g, contact time: 2 h, solid to liquid ratio (s/l): 10 g $L^{-1}$, Initial MB dye concentration 100 mg $L^{-1}$).

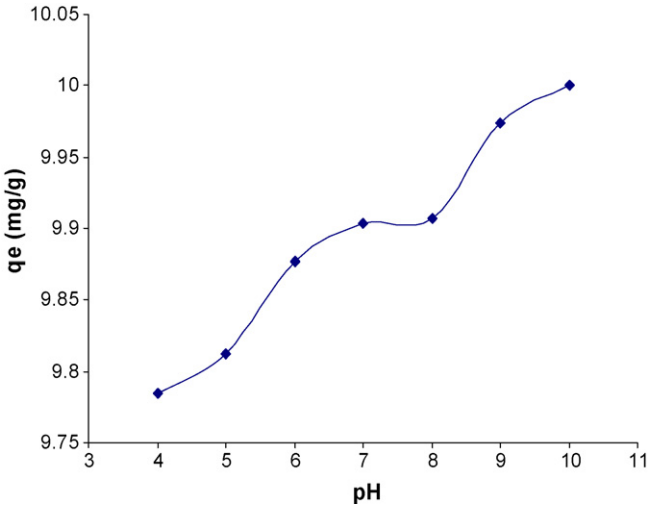


**Fig. 7.** Effect of pH on MB dye adsorption onto DPS adsorbent (initial MB dye concentration: 100 mg $L^{-1}$, contact time: 2 h).

small increase in adsorption capacity of DPS adsorbent from 9.78 to 10.00 mg $g^{-1}$ as pH was increased from 4 to 10. Similar observation was made by Han et al. [33]. This may suggest that the adsorption of MB dye onto DPS adsorbent may not be pH dependent.

pH is, also, known to affect the structural stability of MB dye, and therefore, its colour intensity. Hence, the effect of pH was studied with blank solutions of MB dye of concentration 100 mg $L^{-1}$ having natural pH 7.04. The solution was kept for 2 h, after which the absorbance of the solution at $\lambda = 668$ nm was found out (see Appendix A: Supplementary data for the FTIR plot of MB dye). It was found that the colour is stable in the pH range of 5–7. However, apart from effect of pH study all other studies in this work were carried out at the natural pH of the dye solution.

### 3.5. Effect of initial MB dye concentration

Table 2 shows the Langmuir and Freudlich parameters for the adsorption of MB dye on DPS adsorbent. Increasing initial MB dye concentration from 10 to 400 mg $L^{-1}$ increased the amount of MB adsorbed on DPS adsorbent from 0.98 to 39.56 mg $g^{-1}$. Han et al. [33], also observed similar trend when they adsorbed MB dye on wheat husk. The Langmuir maximum adsorption capacity ($Q^o$) of 1250 mg $g^{-1}$ (Table 2). Hameed [6] obtained 555.557 mg $g^{-1}$ when he used boiled *Carica papaya* seeds for the adsorption of MB dye. The Langmuir adsorption capacity for the undeffated *Carica papaya* seeds (UDPS) was 769.23 mg $g^{-1}$ (Table 2). This suggests that the presence of some oils and fat may have blocked some useful active site on the *Carica papaya* seeds. It is therefore, important that *Carica papaya* seeds be first defatted before use for adsorption purpose. More importantly, is the usefulness of the lipids from the seeds for both medicinal and nutritional purposes by man as mentioned earlier [12].

**Table 2**
Langmuir and Freudlich parameters for the adsorption of MB dyes onto DPS adsorbent.

| | $Q^o$ (mg $g^{-1}$) | $b$ (L $g^{-1}$) | $r^2$ |
|---|---|---|---|
| Langmuir isotherm constants | | | |
| Undefatted Carica p. | 769.23 | 0.0122 | 0.9903 |
| DPS adsorbent | 1250 | 0.0046 | 0.9932 |
| Particle size (μm) | $Q^o$ (mg $g^{-1}$) | $b$ (L $g^{-1}$) | $r^2$ |
| Effect of DPS Particle size (Langmuir plots) | | | |
| 75 | 256.41 | 1.00 | 0.9970 |
| 300 | 18.30 | 1.00 | 0.9915 |
| 500 | 17.57 | 1.00 | 0.9984 |
| 750 | 17.45 | 1.00 | 0.9988 |
| DPS adsorbent | $Q^o$ (mg $g^{-1}$) | $b$ (L $g^{-1}$) | $r^2$ |
| Effect of temperature (Langmuir plots) | | | |
| 298 K | 1250 | 0.0046 | 0.9932 |
| 313 K | 217.39 | 0.024 | 0.9944 |
| 323 K | 100.00 | 0.041 | 0.9865 |
| | $1/n$ | $k_f$ (mg $g^{-1}$) | $r^2$ |
| Freudlich isotherm constants | | | |
| Undefatted Carica p. | 0.107 | 1.00 | 0.9903 |
| DPS adsorbent | 0.872 | 6.16 | 0.9649 |

However, the percentage of MB dye adsorbed was within the range of 97.5–98.9 and increased when initial MB dye concentration was increased from 10 to 400 mg $L^{-1}$. The results obtained by Hameed [6], for the adsorption of MB dye onto boiled *Carica papaya* seeds indicated a decrease in percentage MB dye adsorbed with increasing initial MB concentration. Furthermore, it was observed that in the adsorption of MB dye onto DPS adsorbent there was the onset of equilibrium after 20 min of the adsorption process. The equilibrium adsorption capacity of DPS adsorbent for MB dye increased from 0.98 to 39.56 mg $g^{-1}$, with increase in the initial MB dye concentration from 10 to 400 mg $L^{-1}$.

The essential characteristics of a Langmuir isotherm can be expressed in terms of a dimensionless separation factor, $R_L$ [34] which describes the type of isotherm and is defined by:

$$R_L = \frac{1}{1 + K_L C_0} \tag{15}$$

where $R_L$ is a dimensionless separation factor, $C_0$ is initial MB dye concentration (mg $L^{-1}$) and $K_L$ is Langmuir constant (L $mg^{-1}$). The parameter $R_L$ indicates the shape of the isotherm accordingly:

| values of $K_L$ | type of isotherm |
|---|---|
| $R_L > 1$ | unfavorable |
| $R_L = 1$ | linear |
| $0 < R_L < 1$ | favorable |
| $R_L = 0$ | irreversible. |

Fig. 8 shows the plot of $R_L$ against $C_0$. The values of $R_L$ for $C_0 = 10$, 50, 100, 200, 300 and 400 mg $L^{-1}$ were found to be 0.956, 0.814, 0.687, 0.523, 0.422 and 0.354, respectively. The values of $R_L$ obtained

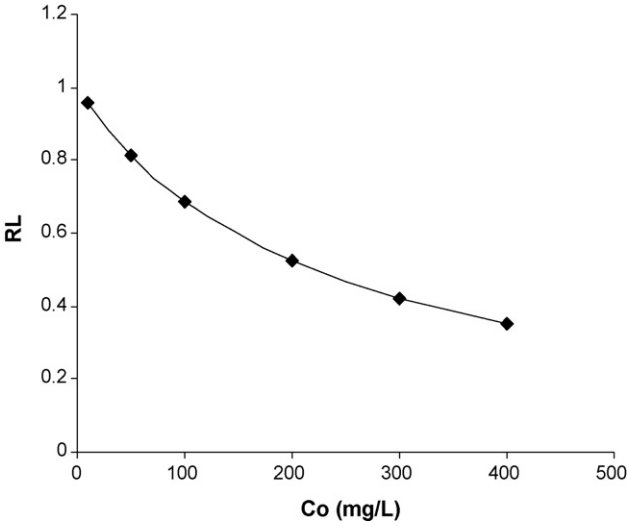


**Fig. 8.** Plot of separation factor $R_L$ versus initial MB dye concentration for DPS adsorbent.

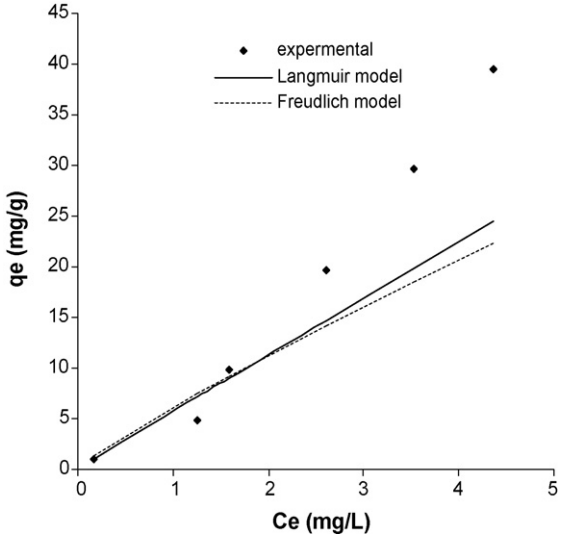


**Fig. 9.** Langmuir and Freudlich model plots for the adsorption of MB dye onto DPS adsorbent.

were found to be less than 1 and decreased with increasing initial concentration of MB dye. This confirms that the adsorption of MB dye onto DPS adsorbent is favourable. The values of $1/n$ were also found to be <1 showing; again that the adsorption is favourable [35].

Fitting experimental data to nonlinear Langmuir and Freudlich models using nonlinear regression suggests that both models showed very good fit to the experimental at low concentrations of MB dye and deviated at concentrations above 100 mg $L^{-1}$ (Fig. 9). Using the nonlinear chi-square equation as shown in Eq. (14) we observed that equilibrium data showed better fit to Langmuir model than to Freudlich model with Langmuir model having a $\chi^2$ value of 11.45 and Freudlich model having a $\chi^2$ value of 14.94.Varying the particle sizes of DPS adsorbent from 75 to 750 μm showed that DPS had a reduced adsorption capacity for the adsorption of MB dye (Table 2). From the surface chemistry study (based on Boehm titration method) of the various particle sizes; 75, 300, 500 and 750 μm, they were observed to have $0.525 \pm 0.106$, $0.392 \pm 0.03$, $0.267 \pm 0.07$ and $0.152 \pm 0.091$ mequiv. $g^{-1}$ total acidic functional groups, respectively, comprising of lactonic, phenolic and carboxylic groups. The total basic functional groups on the various particle sizes of DPS adsorbent were calculated to be $0.150 \pm 0.009$, $0.212 \pm 0.024$, $0.211 \pm 0.107$ and $0.150 \pm 0.001$ mequiv/g for 75, 300, 500, 750 μm of DPS adsorbent respectively (Fig. 5). This may suggest that increasing surface area as a result of decreasing particle size and increasing amount of acidic functional groups with decreasing particle size have played a role in the observed adsorption trend for these particle sizes of DPS adsorbent. Moreso, it was observed that the largest fraction (750 μm) was a dark brown hard coating of the DPS adsorbent while the smallest fraction was a very fine milky coloured powder. From the adsorption capacity results of the crushed DPS adsorbent and that from the various particle sizes of the adsorbent it is suggestive that the whole component of the DPS adsorbent plays a role in the adsorption of MB dye from solution.

### 3.6. Kinetic study

The batch experiments carried out to study the relationship between contact time and MB dye adsorbed by DPS showed that the equilibrium time was virtually reached in 20 min at various initial MB dye concentrations. Fig. 10 shows the effect of initial MB dye concentration on the adsorption capacity of DPS at different contact

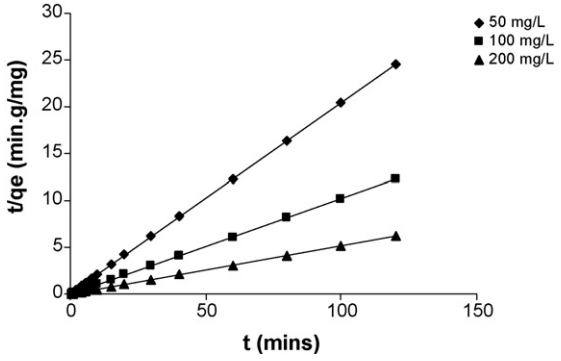


**Fig. 10.** Plot of pseudo-second-order kinetics for the adsorption of MB dye onto DPS adsorbent (initial MB dye concentration: 50, 100 and 200 mg $L^{-1}$, solid to liquid ratio (s/l): 10 g $L^{-1}$).

times. The observed adsorption capacity of DPS varied with varying initial MB dye concentration. From data in Table 3, the pseudo-first-order rate constant was found to increase with increasing initial MB dye concentration. The pseudo-second-order rate constant and adsorption capacity of DPS were observed to follow same trend.

It was observed also that the adsorption process was a very fast one because at 30 s the percentage adsorbed was over 95% (plot not shown). The presence of multiple functional groups and lone pair of electrons on DPS adsorbent might be responsible for this. This relatively rapid MB dye uptake suggests that the adsorption process occurs mainly on the surface of DPS. The uptake of adsorbate by biosorbents has been observed to occur in two stages: the first rapid and quantitatively predominant and the second slower and quantitatively insignificant, has been extensively reported in literature [36]. The rapid adsorption of MB dye by DPS is probably due to the abundant availability of active sites on the biomass, and the perceived porus and mesh structure of DPS which provides ready access and large surface area for the adsorption of MB dye on the binding sites [37]. This very rapid adsorption of MB dye by DPS adsorbent is reflected in the high initial sorption rate, $h$, for the various initial concentrations of MB dye as shown in Table 3. It has been observed that the adsorption of MB dye onto DPS adsorbent is quite faster than on boiled *Carica papaya* seeds. While the rate constant for adsorption of 50 mg $L^{-1}$ of MB dye onto DPS was 0.706 g $mg^{-1}$ $min^{-1}$ (this study) that for boiled *Carica papaya* at same concentration was 0.092 g $mg^{-1}$ $min^{-1}$ [6].

The relationship between $q_e$, $k$ and $h$ and initial MB dye concentration are given by the equations.

$$q_e = 2.0028C_0 - 0.1299 \quad r^2 = 1.0000 \tag{16}$$

**Table 3**
Kinetic parameters for the kinetic models in the adsorption of MB dye by DPS adsorbent.

| Kinetic model | Initial MB concentration (mg $L^{-1}$) | | |
|---|---|---|---|
| | $C_i = 50$ | $C_i = 100$ | $C_i = 200$ |
| Pseudo-first-order | | | |
| $k_1$ ($min^{-1}$) | 0.0342 | 0.0343 | 0.0490 |
| $r^2$ | 0.9850 | 0.7783 | 0.7397 |
| Pseudo-second-order | | | |
| $q_e$ (mg $g^{-1}$) | 4.91 | 9.80 | 19.42 |
| $k_2$ (g $mg^{-1}$ $min^{-1}$) | 0.71 | 1.20 | 1.33 |
| $h$ (mg $g^{-1}$ $min^{-1}$) | 17.01 | 114.94 | 500 |
| $r^2$ | 1.0000 | 1.0000 | 1.0000 |
| Bangham's kinetic equation | | | |
| $k_o$ (g) | 11.34 | 11.03 | 10.94 |
| $\alpha$ | 0.0155 | 0.0109 | 0.0069 |
| $r^2$ | 0.9916 | 0.9108 | 0.8118 |

**Table 4**
Thermodynamic data for the adsorption of MB dye onto DPS adsorbent.

| Concentration ($mg\,L^{-1}$) | $-\Delta H$ ($kJ\,mol^{-1}$) | $-\Delta S$ ($J\,mol^{-1}$) | $r^2$ | $-\Delta G$ ($kJ\,mol^{-1}$) | | |
|---|---|---|---|---|---|---|
| | | | | 298 K | 313 K | 323 K |
| 10 | 10.35 | 19.95 | 0.8304 | 4.33 | 4.33 | 3.77 |
| 50 | 17.71 | 47.48 | 0.7068 | 3.36 | 3.38 | 2.03 |
| 100 | 11.70 | 23.58 | 0.6567 | 4.53 | 4.72 | 3.83 |
| 200 | 9.31 | 14.55 | 0.9437 | 5.01 | 4.65 | 4.68 |
| 300 | 9.69 | 14.97 | 0.9246 | 5.28 | 4.88 | 4.94 |

$$k = 4.0199C_0 - 0.9415 \quad r^2 = 1.0000 \tag{17}$$

$$h = 3.3100C_0 - 175.52 \quad r^2 = 0.9804 \tag{18}$$

From the double logarithmic plots made using the Bangham's equation shown in Eq. (3) (plots not shown) on experimental data, it was also observed that with increasing initial concentration of MB dye there was an increasing deviation from linearity. This is also shown by the $r^2$ values for the various initial MB dye concentration in Table 3. This suggests that the mechanism of the adsorption of MB dye on DPS adsorbent may not strictly be via the pores in the adsorbents but there could also be the contribution of film diffusion, both occurring to varying extents during the adsorption process [35]. From the $r^2$ values (Table 3) it was observed that the pseudo-second-order kinetic model best describe the kinetic data obtained.

### 3.7. Effect of temperature

The different Langmuir parameters for the adsorption of MB onto DPS at 298, 313 and 323 K were obtained using Eq. (2) and are shown in Table 2. It is observed that increasing temperature reduced the adsorption capacity of DPS adsorbent for MB dye.

The enthalpy of the adsorption $\Delta H$ is a measure of the energy barrier that must be overcome by reacting molecules [38]. The values for $\Delta H$ were found to be in the range of 17.71–9.31 $kJ\,K^{-1}\,mol^{-1}$ and were all negative. This suggests that the adsorption reaction of MB dye onto DPS is exothermic in nature meaning that increasing temperature will not favour the adsorption of the dye onto DPS adsorbent. Although $\Delta H$ did not follow a particular trend with increasing initial MB concentration, it was observed that it generally decreased with increase in initial MB dye concentration (Table 4).

The value of $\Delta S$ is an indication of whether or not the adsorption reaction is by associative or dissociative mechanism. The entropy measures the width of the saddle point of the potential energy surface over which reactant molecule must pass as activated complexes [38]. Entropy change $>-10\,J\,K^{-1}\,mol^{-1}$ generally implies dissociative mechanism [39]. Entropy values obtained in this study (Table 4) are below this value. This could suggest an associative mechanism of adsorption of MB dye onto DPS adsorbent. The uptake by red mud of Rhodamine B, fast green, and methylene blue were observed to be exothermic, with a negative entropy change [40].

$\Delta G$, values obtained were all small and negative which suggests that the adsorption of MB dye onto DPS adsorbent is spontaneous and that the adsorption reaction between MB dye and DPS adsorbent is thermodynamically feasible. $\Delta G$, was observed to general decrease with increasing temperature from 298 to 323 K but increased slightly with increasing initial MB dye concentration.

### 3.8. Mechanism of adsorption

From the Fourier transformed infrared (FT-IR) studies of DPS, it was observed that the acidic groups were more than the basic and may have been basically responsible for the adsorption of MB dye onto DPS adsorbent in the following manner:

For the phenolics it is

$$S\text{–}OH + MB^+ \rightleftharpoons S\text{–}O\text{–}MB + H^+$$

For carboxylic acid

$$S\text{–}COOH + MB^+ \rightleftharpoons S\text{–}COOMB + H^+$$

The lone pair of electrons on the Lactones may have been used to adsorb MB dye from aqueous solution.

### 3.9. Optimization of data

#### 3.9.1. Multistage batch adsorption design

Consider a volume of wastewater which contains an impurity/adsorbate of interest at a very dilute concentration of $C_0$ ($mg\,L^{-1}$) which is to be reduced to a concentration of $C_f$ ($mg\,L^{-1}$) by the adsorption onto $M$ (g) of crushed DPS adsorbent. The adsorbent is initially without any adsorbate. The adsorption isotherm is known to follow Henry's law and is given by:

$$q_e = KC_e \tag{19}$$

where $q_e$ is the amount of adsorbate on the adsorbent ($mg\,g^{-1}$) at equilibrium, $C_e$, the amount of adsorbate left in solution at equilibrium ($mg\,L^{-1}$) and $K$ is the equilibrium constant ($L\,g^{-1}$).

It is assumed that water is not adsorbed and since the adsorbate is low, the volume of the solution does not change. The mass balance for the adsorbate is therefore as follows:

$$V(C_0 - C_e) = Mq_e \tag{20}$$

if the adsorbent were not initially free from the adsorbate but had been regenerated to a residual loading of $q_o$ then it would be necessary to replace the right hand side of Eq. (19) with $M(q_e - q_o)$.

Simultaneous solution of Eqs. (1) and (20) gives the mass of the adsorbent required to effect the purification:

$$M = \frac{V}{K}\left(\frac{C_0}{C_e} - 1\right) \tag{21}$$

Eq. (20) shows that the mass of adsorbent required can be reduced if an adsorbent with a higher equilibrium constant is used. Eq. (21) can rearranged to give a linear relationship between $q_e$ and $C_f$.

$$q_e = \frac{V}{M}(C_0 - C_e) \tag{22}$$

If the adsorbent was regenerated before reuse then the linear relationship would be:

$$q_e = \frac{V}{M}(C_0 - C_e) = q_o \tag{23}$$

When a large amount of the adsorbent is required for adsorption of a certain adsorbate consideration should be given to using multiple batch system. For example, one way of reducing the amount of adsorbent required is to carry out batch adsorption of the adsorbate in two-steps as shown schematically in Fig. 11. In this two step batch adsorption system, the total adsorbent is split arbitrarily into two parts $M_1$ and $M_2$. The feed is first contacted with a fresh batch of adsorbent and the adsorbate concentration is reduced to $C_1$. After separation of the fluid from the adsorbent in the first stage

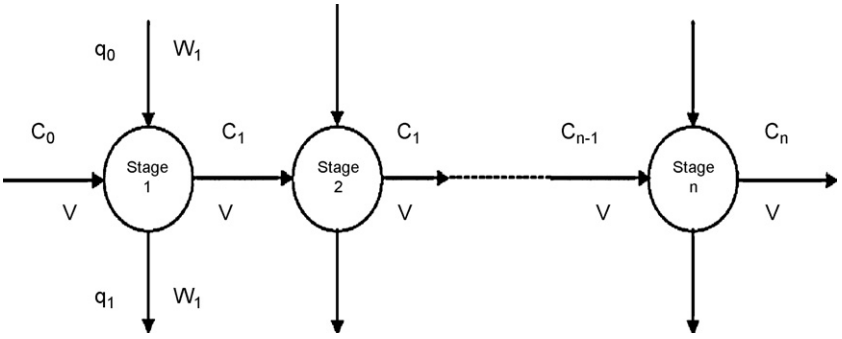


**Fig. 11.** Schematic diagram for a multistage batch adsorber.

the fluid is contacted with a further fresh portion of the adsorbent. In multibatch systems subsequent batch of the adsorbent removes les and less amount of the adsorbate as the adsorbate concentration decreases.

Simultaneous solution of the adsorbate mass balance with the equilibrium relationship for the first batch vessel yields $M_1$:

$$M_1 = \frac{V}{K}\left(\frac{C_0}{C_1} - 1\right) \tag{24}$$

Here $q_1$ (amount adsorbed after stage 1 adsorption) is in equilibrium with intermediate concentration $C_1$. Simultaneous solution of the adsorbate mass balance with the equilibrium relationship for the second batch vessel yields $M_2$:

$$M_2 = \frac{V}{K}\left(\frac{C_1}{C_e} - 1\right) \tag{25}$$

For the total mass of the adsorbent to be a minimum, the differential of $(M_1 + M_2)$ with respect to the intermediate concentration $C_1$ needs to be zero. Thus, it can be shown that:

$$C_1 = (C_0 C_e)^{0.5} \tag{26}$$

Substitution of $C_1$ from Eq. (26) into Eqs. (24) and (25) shows that the minimum amount of adsorbent for the purification is given when:

$$M_1 = M_2 = \left[\frac{V}{k}\left(\frac{C_0}{C_e}\right)^{0.5} - 1\right] \tag{27}$$

For a multistage process involving $N$ stages the general result for a linear isotherm is:

$$\sum(M_1 + M_2 + M_3 \ldots M_N) = \frac{NV}{K}\left[\left(\frac{C_0}{C_e}\right)^{1/N} - 1\right] \tag{28}$$

Comparing Eq. (27), when $N = 2$ with Eq. (28) suggest that by splitting the adsorbent into two equal amounts the total amount of adsorbent required for the given purification is reduced from that required when all the adsorbent is used in one stage. Table 5 shows the total amount of DPS adsorbent required for the adsorption of 99% MB dye from 100 mg $L^{-1}$ of the dye in various volumes of aqueous solution.

Let us consider the optimization of the number of adsorption stages for the batch adsorption of 100 mg $L^{-1}$ of MB dye from known volume of dye and the amount of DPS required for each stage if $M_1 = M_2 \ldots = M_N$ using Eq. (27). Plots showing the optimum amount of adsorbent dose and the corresponding optimum adsorption stages required for the removal of 99% of MB dye from various volumes of influent containing 100 mg $L^{-1}$ of MB dye are shown in Figs. 12 and 13. From Table 5 it was observed that increasing volume of influent requires increasing adsorbent dosage. The optimum number of stages of adsorption decreased with increasing volume of influent (Table 5). For example, five stages and a total of 0.048 kg of DPS adsorbent are required for the removal of 99% of 100 mg $L^{-1}$ MB dye present in 5 L of aqueous solution. For 10,000 L (10 $m^3$), five adsorption stages and a DPS adsorbent dose of 21003.82 g for each of the five stages (Table 6) are required to remove 99% of MB dye from the aqueous solution containing 100 mg $L^{-1}$ of MB dye. However, for volume of influent <2.5 L, adsorption efficiency of DPS adsorbent increased with increasing number of stages until at some stages no adsorption was required. For example, from Table 5, it was observed that further adsorption at stage 6 was unnecessary for the removal of 99% of MB dye from an aqueous solution containing 0.5 L of 100 mg $L^{-1}$ of the dye. For 1 L adsorption was sufficient at the 24th stage (data not shown).

**Table 5**
Optimized data for the total amount of DPS required for the adsorption of 99% of 100 mg $L^{-1}$ MB dye from various volumes of aqueous solution.

| No. of stages | Volume of aqueous solution containing 100 mg $L^{-1}$ of MB dye | | | | | | | | | | | | |
|---|---|---|---|---|---|---|---|---|---|---|---|---|---|
| | 0.5 L | 1 L | 2.5 L | 5 L | 10 L | 50 L | 100 L | 500 L | 1000 L | 1500 L | 2000 L | 2500 L | 10000 L |
| Total amount of DPS (g) required to adsorb 99% of 100 mg $L^{-1}$ MB dye in aqueous solution | | | | | | | | | | | | | |
| 2 | 6.36 | 14.72 | 39.81 | 81.62 | 165.24 | 834.22 | 1670.43 | 8360.17 | 16722.34 | 25084.51 | 33446.68 | 41808.84 | 167241.40 |
| 3 | 2.82 | 8.64 | 26.11 | 55.21 | 113.42 | 579.12 | 1161.23 | 5818.17 | 11640.95 | 17462.92 | 23284.89 | 29106.87 | 116438.10 |
| 4 | 1.29 | 6.58 | 22.44 | 48.89 | 101.77 | 524.87 | 1053.74 | 5284.70 | 10573.4 | 15862.1 | 21150.80 | 26439.50 | 105770.00 |
| 5 | 0.25 | 5.50 | 21.26 | 47.51 | 100.02 | 520.12 | 1045.24 | 5246.21 | 10497.41 | 15748.61 | 20999.82 | 26251.02 | 105019.10 |
| 6 | 0 | 4.81 | 21.02 | 48.05 | 102.09 | 534.47 | 1074.95 | 5398.73 | 10803.45 | 16208.17 | 21612.9 | 27017.62 | 108088.50 |
| 7 | 0 | 4.30 | 21.25 | 49.51 | 106.01 | 558.07 | 1123.14 | 5643.68 | 11294.37 | 16945.05 | 22595.73 | 28246.42 | 113006.70 |
| 8 | 0 | 3.90 | 21.74 | 51.48 | 110.96 | 586.81 | 1181.62 | 5940.11 | 11888.22 | 17836.33 | 23784.44 | 29732.55 | 118954.20 |
| 9 | 0 | 3.55 | 22.38 | 53.77 | 116.54 | 618.70 | 1246.40 | 6267.99 | 12545.04 | 18822.07 | 25099.09 | 31376.11 | 125530.80 |
| 10 | 0 | 3.25 | 23.13 | 56.27 | 122.53 | 652.66 | 1315.31 | 6616.57 | 13243.14 | 19869.72 | 26496.29 | 33122.86 | 132521.40 |
| 11 | 0 | 2.98 | 23.95 | 58.90 | 128.81 | 688.04 | 1387.07 | 6979.37 | 13969.73 | 20960.09 | 27950.46 | 34940.82 | 139796.30 |
| 12 | 0 | 3.78 | 27.46 | 66.91 | 145.82 | 777.11 | 1566.22 | 7879.09 | 14716.78 | 22081.17 | 29445.56 | 36809.95 | 147275.60 |
| 13 | 0 | 2.49 | 25.73 | 64.46 | 141.92 | 761.60 | 1536.22 | 7733.01 | 15479.03 | 23225.04 | 30971.06 | 38717.07 | 154907.30 |
| 14 | 0 | 2.27 | 26.67 | 67.33 | 148.67 | 799.35 | 1612.69 | 8119.45 | 16252.91 | 24386.36 | 32519.81 | 40653.27 | 162655.10 |
| 15 | 0 | 2.05 | 27.63 | 70.25 | 155.51 | 837.54 | 1690.08 | 8510.38 | 17035.78 | 25561.17 | 34086.56 | 42611.94 | 170492.80 |
| 20 | 0 | 1.05 | 32.64 | 85.27 | 190.55 | 1032.74 | 2085.47 | 10507.35 | 21034.69 | 31562.04 | 42089.39 | 52616.73 | 157895.20 |

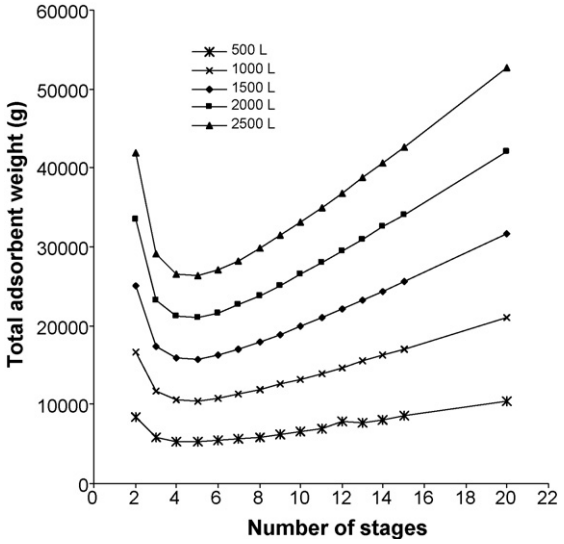


**Fig. 12.** Plots of optimization data for number of stages and total adsorbent weight for the adsorption of 99% of 100 mg $L^{-1}$ MB dye onto DPS adsorbent from various volumes.

### 3.9.2. Optimization of contact time for a multistage batch adsorption process

Although we know the amount of the adsorbent needed for adsorption of the adsorbate and the optimum number of stages required for the most efficient adsorption process, yet the time for the adsorption process for each stage is critical both in the design of the adsorption equipment and its application on a large scale.

From data above, let us consider the minimum contact time required for the removal of 99% MB dye from 10 $m^3$ of 100 mg $L^{-1}$ of the dye in five stages of a batch adsorption process.

Kinetic equations can be used to predict the design of *N*-stage batch sorption systems. The basis of this model is now discussed. A schematic diagram for an *N*-stage adsorption system is shown in Fig. 11.

The solution to be treated contains *L* $dm^3$ solution and the MB dye concentration is reduced for each stage from $C_0$ to $C_1$ mg $dm^{-3}$ [41], $C_1$ to $C_2 \ldots C_m - C_n$. where $C_m$ is equilibrium concentration of MB dye in previous adsorption stage (mg $L^{-1}$) and $C_n$ is final con-

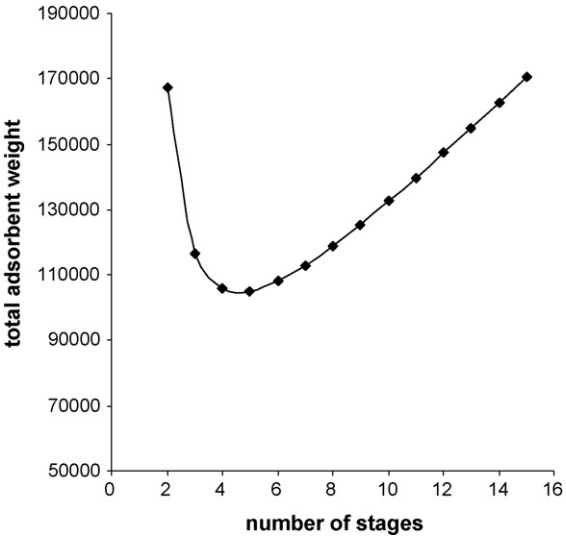


**Fig. 13.** Plots of optimization data for number of stages and total adsorbent weight for the adsorption of 99% of 100 mg $L^{-1}$ MB dye onto DPS adsorbent from 10 $m^3$.

**Table 6**
Optimized data for the amount of DPS required for each stage of the adsorption of 99% of 100 mg $L^{-1}$ MB dye from various volumes of aqueous solution.

| Volume (L) | 2 stages | 3 stages | 4 stages | 5 stages | 6 stages | 7 stages | 8 stages | 9 stages | 10 stages | 11 stages | 12 stages | 13 stages | 14 stages | 15 stages | 20 stages |
|---|---|---|---|---|---|---|---|---|---|---|---|---|---|---|---|
| Amount of DPS (g) required to adsorb 99% of 100 mg $L^{-1}$ MB dye in aqueous solution for each stage ($M_1 = M_2 \ldots = -M_n$) | | | | | | | | | | | | | | | |
| 0.5 | | 3.18 | 0.94 | 0.32 | 0.05 | 0 | 0 | 0 | 0 | 0 | 0 | 0 | 0 | 0 | 0 |
| 1 | 7.36 | 2.88 | 1.64 | 1.10 | 0.80 | 0.61 | 0.49 | 0.39 | 0.33 | 0.27 | 0.23 | 0.19 | 0.16 | 0.14 | 0.05 |
| 2.5 | 19.91 | 8.70 | 5.61 | 4.25 | 3.50 | 3.04 | 2.72 | 2.49 | 2.31 | 2.18 | 2.07 | 1.98 | 1.90 | 1.84 | 1.63 |
| 5 | 40.81 | 18.41 | 12.22 | 9.50 | 8.01 | 7.07 | 6.44 | 5.97 | 5.63 | 5.35 | 5.14 | 4.96 | 4.81 | 4.68 | 4.26 |
| 10 | 82.62 | 37.81 | 25.44 | 20.00 | 17.02 | 15.14 | 13.87 | 12.95 | 12.25 | 11.71 | 11.27 | 10.92 | 10.62 | 10.37 | 9.53 |
| 50 | 417.11 | 193.07 | 131.22 | 104.02 | 89.08 | 79.72 | 73.35 | 68.74 | 65.27 | 62.55 | 60.37 | 58.58 | 57.10 | 55.84 | 51.63 |
| 100 | 835.22 | 387.13 | 263.44 | 209.05 | 179.16 | 160.45 | 147.70 | 138.49 | 131.53 | 126.10 | 121.74 | 118.17 | 115.19 | 112.67 | 104.27 |
| 500 | 4180.08 | 1939.66 | 1321.18 | 1049.24 | 899.79 | 806.24 | 742.51 | 696.45 | 661.66 | 634.49 | 612.70 | 594.85 | 579.96 | 567.36 | 525.37 |
| 1000 | 8361.17 | 3880.32 | 2643.35 | 2099.48 | 1800.58 | 1613.48 | 1486.03 | 1393.89 | 1324.31 | 1269.98 | 1226.40 | 1190.70 | 1160.92 | 1135.72 | 1051.74 |
| 1500 | 12542.25 | 5820.97 | 3965.53 | 3149.72 | 2701.36 | 2420.72 | 2229.54 | 2091.34 | 1986.97 | 1905.46 | 1840.10 | 1786.54 | 1741.88 | 1704.08 | 1578.10 |
| 2000 | 16723.34 | 7761.63 | 5287.70 | 4199.96 | 3602.15 | 3227.96 | 2973.06 | 2788.79 | 2649.63 | 2540.95 | 2453.80 | 2382.39 | 2322.84 | 2272.44 | 2104.47 |
| 2500 | 20904.42 | 9702.29 | 6609.88 | 5250.21 | 4502.94 | 4035.20 | 3716.57 | 3486.23 | 3312.29 | 3176.44 | 3067.50 | 2978.24 | 2903.81 | 2840.80 | 2630.84 |
| 10000 | 83620.69 | 38812.69 | 26442.50 | 21003.82 | 18014.75 | 16143.81 | 14869.27 | 13947.87 | 13252.14 | 12708.75 | 12272.97 | 11915.95 | 11618.22 | 11366.19 | 10526.35 |
| 20000 | 167242.40 | 77626.38 | 52886.00 | 42008.64 | 36030.50 | 32288.62 | 29739.55 | 27895.45 | 26505.29 | 25418.61 | 24546.97 | 23832.89 | 23237.44 | 22733.37 | 21053.69 |

centration of MB dye in aqueous solution at final adsorption stage ($mg\,L^{-1}$).

The amount of DPS adsorbent added is $S$ g with solid-phase dye concentration on the DPS adsorbent $q_0$ $mg\,g^{-1}$. Thus, the MB dye concentration on the adsorbent increases from $q_0$ to $q_1$ $mg\,g^{-1}$ adsorbent. The mass balance equation gives.

$$L(C_{i-1} - C_i) = S(q_{t,i} - q_0) \tag{29}$$

With fresh adsorbents being used at each stage, the pseudo-second-order equation can be used to describe equilibrium in the two-stage sorption system [41]. Thus the mass balance equation can be obtained by combining Eqs. (9) and (29):

$$C_i = C_{i-1} - \frac{Skq_{e,i}^2 t_i}{L(1 + kq_{e,i}t_i)} \tag{30}$$

The total amount of MB dye removal can be calculated analytically as follows.

$$\sum_{i=1}^{N} C_{i-1} - C_i = \sum_{i=1}^{N} \frac{100Skq_{e,i}^2 t_i}{LC_0(1 + kq_{e,i}t_i)} \tag{31}$$

where $i$ is the adsorption system number ($i = 1, 2, 3, 4, \ldots, N$).

The MB dye removal, $R_i$, in each stage can be evaluated from the equation as follows:

$$R_i = \frac{100(C_{i-1} - C_i)}{C_0} = \frac{100Skq_{e,i}^2 t_i}{LC_0(1 + kq_{e,i}t_i)} \tag{32}$$

The total removal of MB dye can be calculated analytically as follows:

$$\sum_{i=1}^{N} R_i = \frac{100S}{LC_0} \sum_{i=1}^{N} \frac{kq_{e,i}^2 t_i}{1 + kq_{e,i}t_i} \tag{33}$$

Therefore it is useful for process design purposes if $q_e$ and $k$ can be expressed as a function of $C_0$ for adsorption of MB dye onto DPS adsorbent as follows:

$$q_e = X_{q_e} C_0^{Yq} \tag{34}$$

$$k = X_k C_0^{Yk} \tag{35}$$

Substituting the values of $q_e$ and $k$ from Eqs. (14) and (15) into Eq. (13) gives:

$$R_i = \frac{100S(X_k C_{i-1}^{Y_k})(X_q C_{i-1}^{Yq})^2 t_i}{LC_0[1 + (X_k C_{i-1}^{Yq})t_i]} \tag{36}$$

$$\sum_{i=1}^{N} R_i = \frac{100S}{LC_0} \sum_{i=1}^{N} \frac{(X_k C_{i-1}^{Y_k})(X_q C_{i-1}^{Yq})^2 t_i}{[1 + (X_k C_{i-1}^{Y_k})(X_q C_{i-1}^{Yq})t_i]} \tag{37}$$

Eqs. (33) and (37) can be used to predict the removal of dye at any given initial dye concentration and the reaction time for any multistage system.

When data of $q_e$ and $k$ against initial MB dye concentration, $C_0$, were regressed the following equations were obtained:

$$298\ \text{K} \quad q_e = 0.1015C_0^{0.9919} \quad r^2 = 1.000 \tag{38}$$

$$298\ \text{K} \quad k = 0.1279C_0^{0.4547} \quad r^2 = 0.8690 \tag{39}$$

When Eqs. (38) and (39) were incorporated into Eq. (37) at 298 K the model equation becomes

$$\sum_{i=1}^{N} R_i = \frac{100S}{LC_0} \sum_{i=1}^{N} \frac{(0.1279C_0^{0.4547})(0.1015C_0^{0.9919})^2 t_i}{\left[1 + (0.1279C_0^{0.4547})(0.1015C_0^{0.9919})\right] t_i} \tag{40}$$

Eq. (40) is a valid mathematical model for the calculation of contact time for the second, third, fourth and fifth stages of a five-stage batch adsorption of MB dye from aqueous solution onto DPS adsorbent.

However, from data available from the optimization of number of adsorption stages and amount of adsorbent dose initially carried out suggested that ≈21.00 kg of the DPS adsorbent is required in each stage in a five stage removal of 99% of MB dye from a 10 $m^3$ aqueous solution containing 100 $mg\,L^{-1}$ of the dye solution.

Thus, let us assume that the first stage of the adsorption process has fixed contact times. For this study, a series of contact times from 2 min up to 28 min in a 2 min increment has been considered in stage one of a five-stage adsorption system for the adsorption of MB dye. In the first adsorber, for example, system number 10 implies that the first adsorber contact time is 2 min + (10 − 1)2 min = 20 min since system number 1 represents 2 min contact time in adsorber number 1. Thus, the contact time in the second adsorber, $t_2$, is the time, $T$ min, required to achieve a fixed total percentage of MB dye removal minus the contact time in the first adsorber stage $t_1$, therefore:

$$T = t_1 + t_2$$

For $N$ systems, $t_n$, becomes

$$t_1 = 2 + (N - 1)2 \ldots \text{min}$$

The total batch contact time, $T$, is

$$T = 2 + (N - 1)2 + t_2 \ldots t_n$$

where $n$ is the number of stages.

Let us assume that the percentage removal in stage two is 50%, stage three is 20%, stage four is 20% and stage five is 9% in a 99% removal of 100 $mg\,L^{-1}$ MB dye from 10 $m^3$ aqueous solutions by ≈21 kg of DPS adsorbent in a five stage adsorption process. The various minimum contact times for the various system numbers for each batch adsorption stage are shown Table 7. Fig. 14 shows the plot of contact time and the equivalent system number for the adsorption of 99% MB dye from 100 $mg\,L^{-1}$ of the dye solution at 50%, 20%, 20%, 9% for stages 2, 3, 4, and 5, respectively. From the table it can be seen that optimum contact time (as shown in system number 5) for the adsorption of 99% removal of 100 $mg\,L^{-1}$ MB dye from 10 $m^3$ aqueous solution by DPS adsorbent is 70.11 min with stage one 10 min, stage two 18.80 min, stage three 14.75 min, stage four 13.01 min and stage five 13.54 min. Other varieties of percentage removal for the various stages were further used for optimization. For example, 70%, 10%, 10% and 9%; 50% 30%, 10% and 9%; and 60%, 20%, 10% and 9% MB dye removal for stages 1, 2, 3, 4 and 5, respectively. They all gave optimum contact times that were

**Table 7**
Optimized minimum contact time data (min) for the adsorption of 100 $mg\,L^{-1}$ MB dye from 10 $m^3$ aqueous solution onto 5 kg DPS adsorbent in a 5-stage batch adsorption process.

| Percentage removal mode for stages 1, 2, 3, 4, and 5 respectively | System no. | Stage 1 | Stage 2 | Stage 3 | Stage 4 | Stage 5 | Total |
|---|---|---|---|---|---|---|---|
| 50%, 20%, 20%, 9% | 5 | 10 | 18.80 | 14.75 | 13.01 | 13.54 | 70.11 |
| 50%, 30%, 10%, 9% | 5 | 10 | 18.80 | 13.79 | 14.58 | 13.50 | 70.67 |
| 60%, 20%, 10%, 9% | 5 | 10 | 17.98 | 14.90 | 14.54 | 13.48 | 70.91 |
| 70%, 10%, 10%, 9% | 4 | 8 | 19.25 | 17.40 | 14.34 | 13.38 | 72.38 |

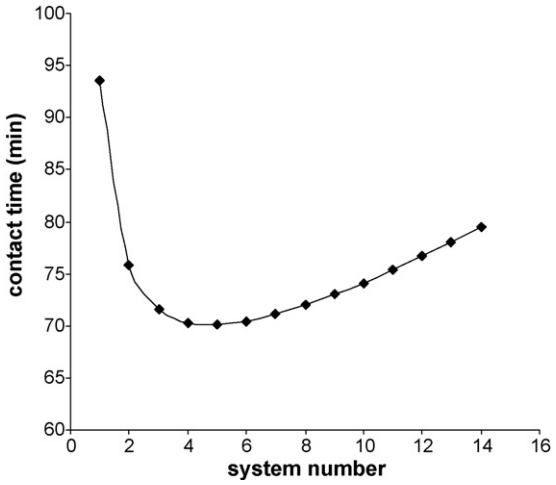


**Fig. 14.** Plots of optimization data contact time and system number for the adsorption of 99% of 100 mg $L^{-1}$ MB dye onto DPS adsorbent from 10 $m^3$.

not statistically different from the initial percentage variation for the various stages (Table 7).

From the optimization results we can suggest the use of ≈21 kg of DPS adsorbent in each stage in a five stage of adsorption for a total of approximately 71 min for the adsorption of 99% MB dye from 10 $m^3$ aqueous solution containing 100 mg $L^{-1}$ of the dye.

## 4. Conclusion

Defatting Carica papaya seed adsorbent (DPS) increased its adsorption capacity for MB dye from 769.23 to 1250 mg $g^{-1}$. FT-IR analysis of the DPS adsorbent suggests the presence of α,β-unsaturated ketone, β-keto (enolic) esters, Lactones, quinones and carboxylic acids which were absent in the Undefatted sample. This was confirmed from chemical analysis of DPS adsorbent. It was observed that acidic groups were responsible for the adsorption of MB dye from aqueous solution.

Increasing dosage of DPS adsorbent increase the percentage Mb dye adsorbed. The adsorption of MB dye onto DPS adsorbent was observed to be very fast which might probably be due to the presence of multiple functional groups present on the adsorbent surface. pH has little effect on the adsorption capacity of DPS for MB dye. This study developed mathematical models for the optimization of number of adsorption stages and contact time for the adsorption of MB dye onto DPS adsorbent. It was observed that five adsorption stages and ≈21 kg of DPS adsorbent is required to remove 99% of 100 mg $L^{-1}$ MB dye from aqueous solution.

## Acknowledgement

The authors wish to acknowledge with thanks the Department of Chemical Sciences, Redeemer's University for the provision of research facilities for this work.

## Appendix A. Supplementary data

Supplementary data associated with this article can be found, in the online version, at doi:10.1016/j.cej.2009.07.012.

## References

[1] A. Mahir, D. Özkan, D. Mehmet, Removal of acid yellow 49 from aqueous solution by adsorption, Fresen. Environ. Bull. 13 (2004) 1112–1121.
[2] T. Robinson, G. McMullan, R. Marchant, P. Nigam, Remediation of dyes in textile effluent: a critical review on current treatment technologies with a proposed alternative, Bioresour. Technol. 77 (2001) 247–255.
[3] K.V. Kumar, K. Porkodi, Batch adsorber design for different solution volume/adsorbent mass ratios using the experimental equilibrium data with fixed solution volume/adsorbent mass ratio of malachite green onto orange peel, Dyes Pigments 74 (2007) 590–594.
[4] I.D. Mall, V.C. Srivastava, N.K. Agarwal, I.M. Mishra, Adsorptive removal of malachite green dye from aqueous solution by bagasse fly ash and activated carbon-kinetic study and equilibrium isotherm analyses, Colloids Surf. A: Physicochem. Eng. Aspects 264 (2005) 17–28.
[5] B. Armagcaronan, O. Özdemir, M. Turan, M. Çelik, Removal of reactive azo dyes by zeolites, J. Chem. Technol. Biotechnol. 78 (2003) 725–732.
[6] B.H. Hameed, Evaluation of papaya seeds as a novel non-conventional low-cost adsorbent for removal of methylene blue, J. Hazard. Mater. 162 (2009) 939–944.
[7] J.P. Morales-Payan, W.M. Stall, Papaya (carica papaya) response to Foliar treatments with organic complexes of peptides and amino acids, Proc. Florida State Hort. Soc. 116 (2003) 30–32.
[8] FAOSTAT. Food and Agricultural Organization of the United Nations. Statistical database, 2003. Agricultural production 2002, FAO, Rome, Italy.
[9] W. Popenoe, Manual of Tropical and Subtropical Fruits, Hafner Press, 1974, pp. 225–269.
[10] J.F. Morton, Fruits of Warm Climates, Creative Resources Systems Inc., 1984, pp. 336–346.
[11] J.A. Samson, Tropical Fruits, 2nd ed., Longman Scientific and Technical, 1986, pp. 256–269.
[12] T. Oduola, F.A.A. Adeniyi, E.O. Ogunyemi, I.S. Bello, T.O. Idowu, H.G. Subair, Toxicity studies on an unripe *Carica papaya* aqueous extract: biochemical and haematological effects in wistar albino rats, J. Med. Plants Res. 1 (2007) 1–4.
[13] R.C. Badami, C.D. Daulatabad, The component acids of *Carica papaya* (caricaceae) seed oil, J. Sci. Food Agric. 38 (1966) 360–366.
[14] T. Puangsri, S.M. Abdulkarim, H.M. Ghazali, Properties of *Carica papaya* L. (papaya) seed oil following extractions using solvent and aqueous enzymatic methods, J. Food Lipids 12 (2005) 62–76.
[15] S. Bashaa, Z.V.P. Murthy, B. Jha, Sorption of Hg(II) onto *Carica papaya*: Experimental studies and design of batch sorber, Chem. Eng. J. 147 (2009) 226–234.
[16] D. Prahas, Y. Kartika, N. Indraswati, S. Ismadji, Activated carbon from jackfruit peel waste by $H_3PO_4$ chemical activation: Pore structure and surface chemistry characterization, Chem. Eng. J. 140 (2008) 32–42.
[17] S.J. Gregg, K.S.W. Sing, The physical adsorption of gases by nonporous solids: the type II isotherm, in: Adsorption, Surface Area and Porosity, Academic Press, London, 1982, pp. 41–110.
[18] D. Graham, Characterization of physical adsorption systems. III. The separate effects of pore size and surface acidity upon the adsorbent capacities of activated carbons, J. Phys. Chem. 59 (1955) 896–900.
[19] Y. Yukselen, A. Kaya, Suitability of the methylene blue test for surface area, cation exchange capacity and swell potential determination of clayey soils, Eng. Geol. 1–2 (2008) 38–45.
[20] Y. Yukselen, A. Kaya, Comparison of methods for determining specific surface area of soils, J. Geotech. Geoenviron. Eng. 132 (2006) 931–936.
[21] P.T. Hang, G.W. Brindley, Methylene blue absorption by clay minerals. determination of surface areas and cation exchange capacities (clay-organic studies xviii), Clays Clay Miner. 18 (1970) 203–212.
[22] P.V. Sivapullaiah, B.G. Prasad, M.M. Allam, Methylene blue surface area method to correlate with specific soil properties, Geotechn. Testing J. (2008), doi:10.1520/GTJ101429.
[23] M.J. Avena, L.E. Valenti, V. Pfaffen, C.P. De Pauli, Methylene blue dimerization does not interfere in surface-area measurements of kaolinite and soils, Clays Clay Miner. 49 (2001) 168–173.
[24] K.R. Hall, L.C. Eagleton, A. Acrivos, T. Vermeulen, Pore and solid diffusion kinetics in fixed-bed adsorption under constant-pattern conditions, Ind. Eng. Chem. Fundam. 5 (1966) 212–213.
[25] S.D. Faust, O.M. Aly, Adsorption Processes for Water Treatment, Butterworths, 1987.
[26] Y.S. Ho, A.E. Ofomaja, Kinetics and thermodynamics of lead ion sorption on palm kernel fiber from aqueous solution, Process Biochem. 40 (2005) 3455–3461.
[27] K.C. Kang, S.S. Kim, J.W. Choi, S.H. Kwon, Sorption of $Cu^{2+}$ and $Cd^{2+}$ onto acid- and base-pretreated granular activated carbon and activated carbon fiber samples, J. Ind. Eng. Chem. 14 (2008) 131–135.
[28] S. Boudesocque, E. Guillon, M. Aplincourt, F. Martel, S. Noël, Use of a low-cost biosorbent to remove pesticides from wastewater, J. Environ Qual. 37 (2008) 631–638.
[29] R.P. Srinivasa, S. Kalyani, R.K. Suresh, A. Krishnaiah, Biosorption of hexavalent chromium from aqueous solution by using prawn pond algae (*Sphaeroplea*), Indian J. Chem. 46A (2007) 284–289.
[30] M. Horsfall Jnr, F.E. Ogban, E.E. Akporhonor, Recovery of lead and cadmium ions from metal-loaded biomass of wild cocoyam (*Caladium bicolor)* using acidic, basic and neutral eluent solutions, Electron. J. Biotechnol. 9 (2006) 152–156.
[31] G. Sreelatha, P. Padmaja, Study of removal of cationic dyes using palm shell powder as adsorbent, J. Environ. Prot. Sci. 2 (2008) 63–71.
[32] D. Lu, Q. Cao, X. Li, X. Cao, F. Luo, W. Shao, Kinetics and equilibrium of Cu(II) adsorption onto chemically modified orange peel cellulose biosorbents, Hydrometallurgy 95 (2009) 145–152.
[33] R. Han, Y. Li, L. Zou, Q. Sheng, J. Cheng, F. Xie, Z. Zhao, Adsorption of methylene blue from aqueous solution by wheat husk in batch mode, in: The 2nd Interna-

tional Conference on Bioinformatics and Biomedical Engineering, 2008. ICBBE 2008, 16–18 May 2008, 2008, pp. 3157–3160.
[34] C. Kaewprasit, E. Hequet, N. Abidi, J.P. Gourlot, Application of methylene blue adsorption to cotton fiber specific surface area measurement: part I. Methodology, J. Cotton Sci. 2 (1998) 164–173.
[35] C. Aharoni, S. Sideman, E. Hoffer, Adsorption of phosphate ions by colloid ion-coated alumina, J. Chem. Technol. Biotechnol. 29 (1979) 404–412.
[36] Y.T. Sag, Kutsal fully competitive biosorption of chromium(VI) and iron(III) ions from binary metal mixtures by *R. arrhizus*: use of the competitive Langmuir model, Process Biochem. 31 (1996) 561–579.
[37] A. Saeed, M.W. Akhter, M. Iqbal, Removal and recovery of heavy metals from aqueous solution using papaya wood as a new biosorbent, Sep. Purif. Technol. 45 (2005) 25–31.
[38] W.P. Jencks, Catalysis in Chemistry and Enzymology, McGraw-Hill, New York, 1969.
[39] K.R. Scheckel, L. Donald, Sparks temperature effects on nickel sorption kinetics at the mineral–water interface, Soil Sci. Soc. Am. J.urnal 65 (2001) 719–728.
[40] V.K. Gupta, I. Ali, V.K. Saini, Suhas, Removal of rhodamine B, fast green, and methylene blue fromwastewater using redmud, an aluminum industrywaste, Ind. Eng. Chem. Res. 43 (2004) 1740–1747.
[41] Y.S. Ho, G. McKay, A two-stage batch sorption optimized design for dye removal to minimize contact time, Trans. IChemE 76B (1998) 313–318.